

Spin Stiffness of Stacked Triangular Antiferromagnets

A. Peles and B.W. Southern*
Department of Physics and Astronomy
University of Manitoba
Winnipeg Manitoba
Canada R3T 2N2
 (Dated: March 22, 2022)

We study the spin stiffness of stacked triangular antiferromagnets using both heat bath and broad histogram Monte Carlo methods. Our results are consistent with a continuous transition belonging to the chiral universality class first proposed by Kawamura.

PACS numbers: 75.40.Cx, 75.40.Mg

I. INTRODUCTION

The magnetic ordering of geometrically frustrated antiferromagnets differs substantially from the conventional magnetic ordering in nonfrustrated magnets^{1,2}. Indeed, the nature of the phase transition in the case of stacked triangular antiferromagnets remains controversial^{3,4,5,6,7,8,9,10,11,12}. The geometry of the stacked triangular lattice has triangles as the elementary units and this arrangement inhibits an anti-parallel alignment of the spins in each triangular layer. Consequently, the system is said to be geometrically frustrated. This frustration leads to a compromise where the spins on each triangle adopt a non-collinear spin ordering at low temperatures. The spins form a planar configuration in which nearest neighbours are oriented at an angle of 120 degrees with respect to one another. The ground state can be described by a matrix like order parameter giving the orientation of each spin on the elementary triangles and forms an SO(3) parameter space¹³. This unusual symmetry of the order parameter and the appearance of 'chiral' degrees of freedom which correspond to the ground state having two possible realizations, left and right handed, lead Kawamura¹⁴ to conjecture the existence of a new chiral universality class. The chiral degrees of freedom are believed to be responsible for the novel critical behaviour but they are not decoupled from the spin degrees of freedom and the two quantities order simultaneously. While recent field-theoretic renormalization group studies of this system using an expansion up to six loops in fixed dimension $d = 3$ indicate the existence of a stable fixed point that corresponds to the proposed chiral universality class^{10,11}, similar analyses using a three loop perturbation technique as well as an epsilon expansion approach to the same order, did not find a stable fixed point and hence exclude the possibility of a continuous phase transition for this frustrated system^{7,8}. Non perturbative RG approaches find that the phase transition is possibly a very weak first order transition with effective critical exponents⁹.

In the present work we use both a standard heat bath Monte Carlo method as well as a recently developed broad histogram method¹⁵ to study the classical isotropic antiferromagnet on this geometry. In particu-

lar, we study the spin stiffness which provides a direct measure of the correlation length exponent ν . The spin stiffness is a convenient quantity to study since it does not require knowledge of the order parameter but does measure the rigidity of the ordered phase against fluctuations. Our results confirm the picture of a continuous transition belonging to a new chiral universality class.

II. MODEL AND METHODS

The model is described by the following Hamiltonian

$$H = - \sum_{i < j} J \vec{S}_i \cdot \vec{S}_j - \sum_{k < l} J' \vec{S}_k \cdot \vec{S}_l. \quad (1)$$

where \vec{S}_i is a classical three component vector of unit length located at the sites i of a hexagonal lattice. The first sum is over nearest neighbours in the triangular planes which interact with an antiferromagnetic coupling $J < 0$ and the second sum is over inter-plane nearest neighbours which are taken to have a ferromagnetic coupling $J' > 0$ with $|J'| = |J| = 1$. Hence all energies and temperatures are measured in units of $|J|$.

We study the response of the system to a virtual twist of the spin system. The spin stiffness, or helicity modulus¹⁶, measures the increase in free energy associated with twisting the order parameter in spin space by imposing a gradient of the twist angle about some axis \hat{n} in spin space along some direction \hat{u} in the lattice. The spin stiffness can be written as a second derivative of the free energy with respect to the strength of the gradient and can be calculated as an equilibrium response function¹⁷. Finite size scaling theory predicts that the spin stiffness should vanish at the critical point with an exponent related to the correlation length exponent.

We calculate the diagonal elements of the spin stiffness tensor corresponding to twists about three principal directions in spin space. If we divide the lattice sites into three equivalent sublattices A, B and C corresponding to the vertices of the elementary triangles, then a chirality vector can be defined to characterize the non-collinear ordering of the spins. The chirality is defined locally for

each upward (downward) triangle by the following expression

$$\vec{K}_\Delta = \vec{S}_A \times \vec{S}_B + \vec{S}_B \times \vec{S}_C + \vec{S}_C \times \vec{S}_A \quad (2)$$

In the ground state, the chirality is uniform and perpendicular to the spin planes. This symmetry of the order parameter suggests that the average chirality di-

rection (\hat{K}) be chosen for one of the principal axes and the other two directions ($\hat{\perp}_1, \hat{\perp}_2$) are chosen to be in the spin plane perpendicular to the average chirality vector such that the three vectors form an orthonormal triad. The spin stiffness component ρ_α at temperature T can be written as¹⁷

$$\rho_\alpha = \frac{1}{N} \sum_{i < j} J_{ij} (\hat{e}_{ij} \cdot \hat{u})^2 \langle S_i^\beta S_j^\beta + S_i^\gamma S_j^\gamma \rangle - \frac{1}{NT} \left\langle \left(\sum_{i < j} J_{ij} (\hat{e}_{ij} \cdot \hat{u}) [S_i^\beta S_j^\gamma - S_i^\gamma S_j^\beta] \right)^2 \right\rangle \quad (3)$$

where $\alpha, \beta, \gamma = \hat{K}, \hat{\perp}_1, \hat{\perp}_2$ and the indices are taken in cyclic order. The twist is taken to be along the \hat{u} direction in the lattice and \hat{e}_{ij} is a unit vector directed along the nearest neighbour bond from site i to j . The angular brackets indicate a thermal average in the canonical ensemble. Since the ground state is a planar spin arrangement, the stiffnesses satisfy a perpendicular axis theorem $\rho_{\hat{K}} = \rho_{\hat{\perp}_1} + \rho_{\hat{\perp}_2}$ at zero temperature. Deviations from this relationship are a measure of fluctuations of spins from the planar order.

We perform numerical simulations using both a conventional Monte Carlo (MC) heat bath method and the more recent broad histogram method (BHM) introduced by Oliveira et. al. The latter method is based on the microcanonical ensemble approach to statistical sampling at fixed energy and allows an accurate estimate of the energy density of states^{15,18,19} $g(E)$. By knowing the density of states $g(E)$ and the microcanonical averages of various quantities $\langle Q \rangle_E$, their temperature dependence can be determined by using the following expression for the canonical averages

$$\langle Q \rangle_T = \frac{\sum_E \langle Q \rangle_E g(E) e^{-E/T}}{\sum_E g(E) e^{-E/T}} \quad (4)$$

In the conventional heat bath method temperature is tuned as an external parameter and number of temperature points is limited by number of computer runs. The BHM method allows us to probe the system in a continuous range of T but requires a large number of energy bins for large system sizes. We simulate spin systems of size $N = L^3$ with $L = 24, 30, 42, 60$ and 66 for the heat bath method and only up to $L = 60$ for the BHM method. Periodic boundary conditions are employed for both methods. We find excellent agreement between these two numerical methods.

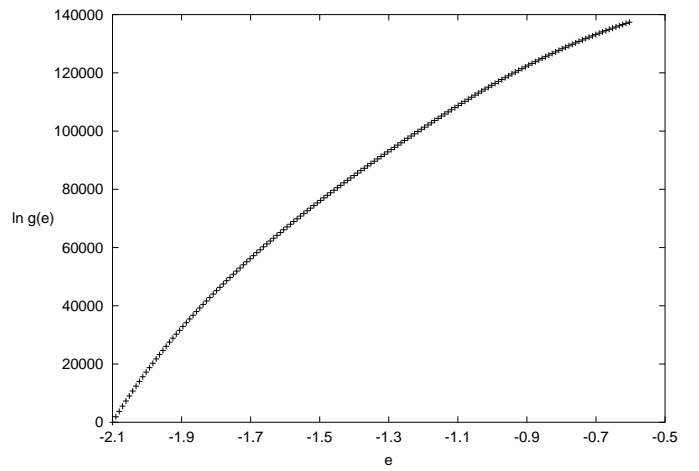


FIG. 1: Natural logarithm of the energy density of states versus the energy per site e for a $42 \times 42 \times 42$ lattice in the range $-2.1 \leq e \leq -0.5$.

III. RESULTS

The broad histogram method(BHM) is based on the relation

$$g(E) \langle N_{up}(E) \rangle = g(E + \Delta E) \langle N_{dn}(E + \Delta E) \rangle \quad (5)$$

where $\langle N_{up}(E) \rangle, \langle N_{dn}(E) \rangle$ are microcanonical averages which measure the number of moves which increase (decrease) the energy by the amount ΔE . Once these microcanonical averages are known, the microcanonical temperature $T_m(E)$ can be determined from

$$\begin{aligned} 1/T_m(E) &\equiv \frac{d \ln g(E)}{dE} \\ &\simeq \frac{1}{\Delta E} \ln \frac{\langle N_{up}(E) \rangle}{\langle N_{dn}(E + \Delta E) \rangle} \end{aligned} \quad (6)$$

and we can then integrate this expression in some range of energy to obtain the energy density of states $\ln g(E)$ as a

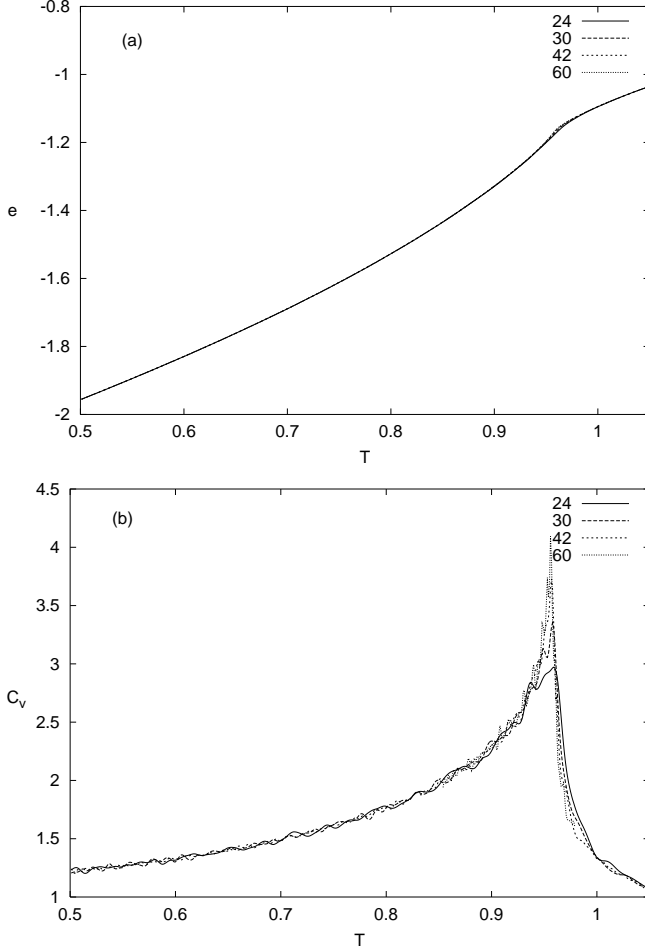


FIG. 2: Energy per site e and specific heat C_v obtained using the BHM method for $L = 24, 30, 42, 60$.

function of E . In our case the energy is a continuous variable and we divide the energy axis into bins of a fixed size $\Delta E = 1.8$ such that $\Delta E \ll E$, where E is total energy of interest. We employ a simple microcanonical dynamics to sample phase space and the energy density of states $g(E)$ (up to a multiplicative constant) is determined using the BHM relation above. One microcanonical sweep consists of a random sweep through the lattice sites and generating a new configuration of the spins by restricting the choice of a new random orientation of the spin at site i with respect to the local field of the nearest neighbours such that the total energy of the system remains within the energy interval $E, E + \Delta E$. At any given value of E , 75 microcanonical sweeps were performed and 25 sample measurements were taken of various thermodynamic quantities such as the energy, specific heat and spin stiffness. Before sampling the next energy interval, 40 initial microcanonical sweeps were performed to avoid correlations. This procedure was repeated using different seeds for random numbers and errors were determined using the standard deviations for these separate measurements.

Figure 1 shows our results for $\ln g(e)$ as a function of

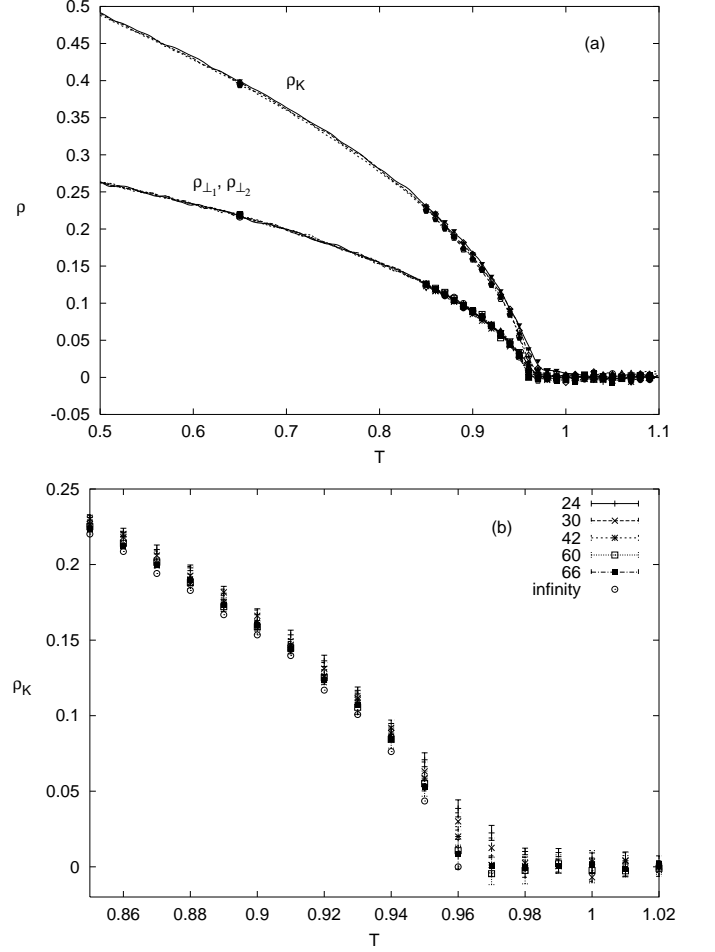


FIG. 3: Spin stiffnesses as a function of T . a) the points indicate the heat bath results and the lines correspond to the BHM results. All three stiffnesses vanish at the same finite temperature near $T \sim .96$. b) the heat bath results for ρ_K in a smaller temperature range show significant finite size effects near T_c .

$e = E/N$ in the case of a $42 \times 42 \times 42$ lattice. The units are arbitrary since we integrate equation (6) starting from $e = -2.1$ and not the ground state value $e_0 = -2.5$. The number of energy bins used for this energy range was 61740. For general values of L , the number of energy bins required to study this same range with the same fixed size of energy bin is $5L^3/6$ and is thus of the same order as the number of sites. When the energy density of states is combined with the microcanonical averages $\langle Q \rangle_E$ for various thermodynamic quantities, we can then plot them as continuous functions of T using equation (4). Figure 2 shows the energy per site and the specific heat obtained using the BHM method for various linear sizes L . The energy displays strong finite size effects near the temperature where the specific heat has a maximum. The figures clearly indicate that a phase transition occurs near $T \sim 0.96$ in agreement with previous MC studies.¹

We have used both the BHM method and a Monte

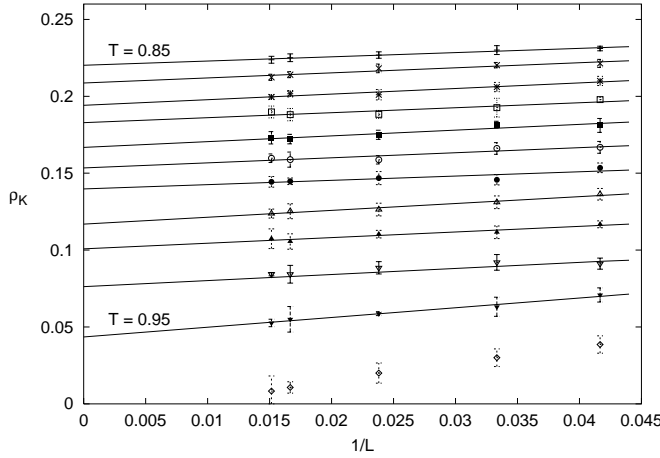


FIG. 4: The same data as in figure 3(b) is plotted as a function of $1/L$ for a set of equally spaced temperatures in the range $.85 \leq T \leq .95$. Extrapolation to the large L limit yields estimates for ρ_K for an infinite lattice.

Carlo heat bath method at fixed values of T to calculate the spin stiffness. In the heat bath method, we discard the first 1000 sweeps and perform 45000 MC steps in each run. Figure 3(a) shows both our heat bath results, indicated by points, and the BHM results, indicated by lines, for the three stiffnesses for various lattice sizes L as a function of the temperature T . The relation $\rho_{\hat{K}} = \rho_{\hat{1}_1} + \rho_{\hat{1}_2}$ is well satisfied for all values of $T < 0.95$ indicating that there is a relatively small deviation from the planar spin configuration. All three stiffnesses are nonzero at low T and vanish near $T \sim .96$ which corresponds to the specific heat divergence in figure 2. Figure 3(b) shows the heat bath data for $\rho_{\hat{K}}$ on an enlarged temperature scale. The stiffnesses clearly show large finite size effects and approach zero near $T \sim .96$. The points labelled infinity are obtained by plotting $\rho_{\hat{K}}$ versus $1/L$ at various values of T and extrapolating to the large L limit as shown in figure 4.

These finite size effects can be used to determine the correlation length exponent ν directly. Finite size scaling considerations for $\rho(T, L)$ predict

$$\rho(T, L) = \frac{1}{L} f(L/\xi) = \frac{1}{L} f(L^{1/\nu} |t|) \quad (7)$$

where t is the reduced temperature. This form suggests that we can plot $L\rho(T, L)$ versus T to identify T_c as the temperature where the curves for different values of L intersect. Figure 5 shows our heat bath results for $L\rho_K$ as a function of T for lattice sizes $L = 24, 30, 42, 60, 66$. Linear interpolations of neighbouring temperature points indicate that the curves intersect at a value of $T_c = 0.958 \pm 0.002$. We have also used our BHM results in the same temperature range and we obtain the same estimate for T_c .

In the limit as $L \rightarrow \infty$, the scaling form predicts $\rho \sim |t|^\nu$. Using the values of the stiffness obtained by extrapolating to large values of L as in figure 4 and then

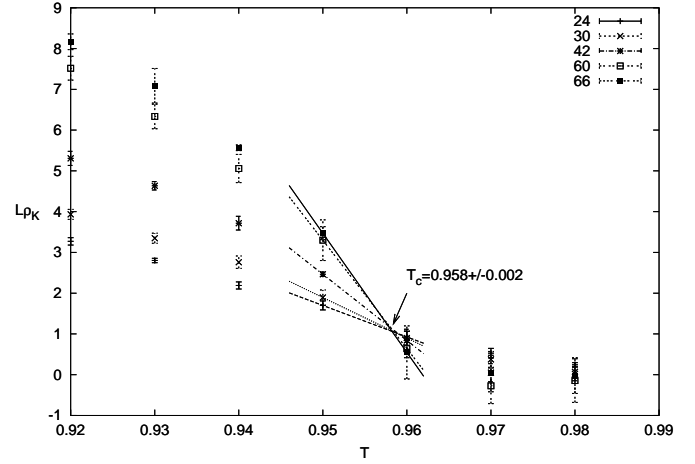


FIG. 5: $L\rho_K$ versus T for various lattice sizes are indicated by the points. The lines are linear interpolations which indicate a unique crossing point at $T_c = 0.958 \pm 0.002$

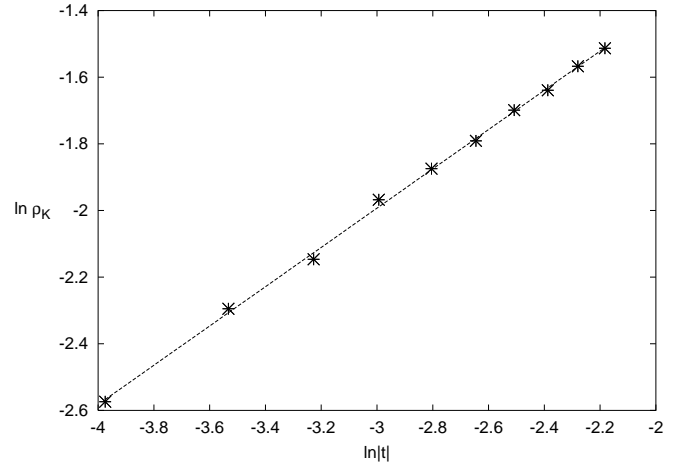


FIG. 6: A $\ln\text{-}\ln$ plot of ρ_K as $L \rightarrow \infty$ versus $|t|$ using the estimated value of T_c yields a value of $\nu = .589 \pm .007$.

plotting these versus $|t|$ on a $\ln\text{-}\ln$ scale, we can obtain an estimate of ν . Figure 6 shows our results for ρ_K which yields the value $\nu = .589 \pm .007$. This value agrees very well with previous Monte Carlo estimates¹ but is slightly larger than the value found by the recent six loop renormalization group calculations in three dimensions.^{10,11}

Figure 7 shows a finite size scaling plot of our stiffness results using the values of T_c and ν quoted above. The data obtained from both the heat bath MC method for sizes $L = 24, 30, 42, 60, 66$ and the BHM method for $L = 24, 30, 42$ collapse very well to a universal function for temperatures below T_c . The value $\nu = .589 \pm .007$ is certainly very different from the value $\nu = 0.7113$ which describes the three dimensional Heisenberg universality class.²⁰

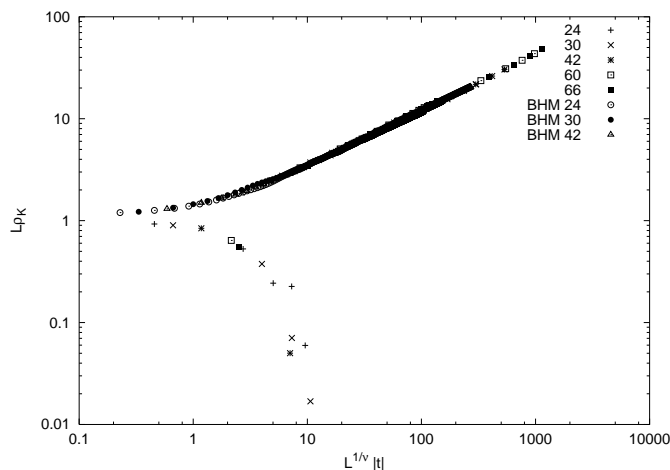


FIG. 7: Finite-size scaling plot of $L\rho_K$ versus $L^{1/\nu}|t|$ produces a universal curve

IV. SUMMARY

We have calculated the spin stiffness of the isotropic Heisenberg antiferromagnet on the stacked triangular geometry using both a MC heat bath and BHM method. The spin stiffness has the advantage that it measures the rigidity of the ordered phase in response to a virtual twist without having to specify the order parameter. The results obtained from both numerical approaches agree and predict a continuous phase transition which belongs to the new chiral universality class proposed by Kawamura.

Acknowledgments

This work was supported by the Natural Sciences and Research Council of Canada and the HPC facility at the University of Manitoba.

-
- * email:souther@cc.umanitoba.ca
- ¹ H. Kawamura, J. Phys.: Condens. Matter. **10**, 4707 (1998).
 - ² H. Kawamura, Can. J. Phys. **79**, 1447 (2001).
 - ³ B. Gaulin, in *Magnetic Systems with Competing Interactions*, edited by H. Diep (World Scientific, 1994), p. 286.
 - ⁴ M. F. Collins and O. A. Petrenko, Can. J. Phys. **75**, 605 (1997).
 - ⁵ H. Kawamura, J. Phys. Soc Jpn. **61**, 1299 (1992).
 - ⁶ A. Mailhot, M. L. Plumer, and A. Caillé, Phys. Rev. B **50**, 6854 (1994).
 - ⁷ S. A. Antonenko and A. I. Sokolov, Phys. Rev. B **49**, 15901 (1994).
 - ⁸ S. A. Antonenko, A. I. Sokolov, and K. B. Varnashev, Phys. Lett. **208A**, 161 (1995).
 - ⁹ M. Tissier, B. Delamotte, and D. Mouhanna, Phys. Rev. Lett. **84**, 5208 (2000), cond-mat/0107183.
 - ¹⁰ A. Pelissetto, P. Rossi, and E. Vicari, Phys. Rev. B **65**, 020403(R) (2001).
 - ¹¹ A. Pelissetto, P. Rossi, and E. Vicari, Phys. Rev. B **63**, 140414(R) (2001).
 - ¹² D. Loison and K. D. Schotte, Eur. Phys. J. B **14**, 125 (2000).
 - ¹³ T. Dombre and N. Read, Phys. Rev. B **39**, 1989 (1989).
 - ¹⁴ H. Kawamura, J. Phys. Soc. Jpn. **54**, 3220 (1985).
 - ¹⁵ P. M. C. de Oliveira, T. J. P. Penna, and H. J. Herrmann, Braz. J. Phys. **26**, 677 (1996), cond-mat/9610041.
 - ¹⁶ M. E. Fisher, M. N. Barber, and D. Jasnow, Phys. Rev. A **8**, 1111 (1973).
 - ¹⁷ B. W. Southern and A. P. Young, Phys. Rev. B **48**, 13170 (1993).
 - ¹⁸ J. D. Muñoz and H. J. Herrmann, in *Computer Simulation Studies in Condensed-Matter Physics XII*, edited by D. Landau (Springer, Berlin, 1999), cond-mat/9810292.
 - ¹⁹ P. M. C. de Oliveira, Eur. Phys. J. B **6**, 111 (1998).
 - ²⁰ M. Campostrini, M. Hasenbusch, A. Pelissetto, P. Rossi, and E. Vicari, Phys. Rev. B **65**, 144520 (2002).